Modeling Injections During April 17-18, 2002

Kristi A. Keller, Michael Hesse, Lutz Rastaetter, Ayris Falasca, Maria M. Kuznetsova, Mei-Ching Fok

Goddard Space Flight Center

Tamas I. Gombosi, Darren L. DeZeeuw

University of Michigan

Abstract

During April 2002, a number of magnetic storm occurred in the magnetosphere, which included a number of interesting features. One of these is injections, observed by geosynchronous satellites on April 17. During the same period, oscillations were also observed in the cross polar cap potential. Using a combination of the BATSRUS global MHD simulation developed by the University of Michigan and Mei-Ching Fok's ring current model, we will examine the relationship between injections in the inner magnetosphere and the underlying magnetospheric dynamics. In particular, we will examine the timing of the oscillations in the cross polar cap potential and injections in the ring current, as well as their causal connection. Our results will be compared to the observations during the period of interest.

BATSRUS Information

- BATSRUS solves the ideal MHD equations using an adaptive mesh. In this run the smallest resolution was 1/8 R_E. After the initial setup, the grid was fixed.
- The box was from –255 to 33 R_E in the GSM x direction and –48 to 48 R_E in the other two directions.
- We used level 2 ACE data and propagated the solar wind data from ACE to 33 R_E using an average velocity.
- The FACs at 4 R_E are mapped along dipole field lines to the ionosphere to calculate the electrostatic potential in the ionosphere.

Fok Model

- The Fok Ring Current Model calculates the evolution of the ring current particle fluxes by solving a bounce-averaged Boltzmann transport equation.
- The model uses a combined convection-diffusion approach included drift, charge exchange, radial and pitch angle diffusion.
- The Fok Ring Current Model uses the ionospheric potential, magnetic field, density and temperature from the BATSRUS model.

Event Introduction

- On April 17, a shock impacted the magnetosphere around 11:08. Around this time increases in the proton fluxes were seen by three geosynchronous satellites.
- After this shock, there was a decrease in the solar wind density and temperature. The proton fluxes seen by three geosynchronous satellites also decreased during this time period.
- Around 15:40, there was an increase in the proton flux seen by LANL-97A.

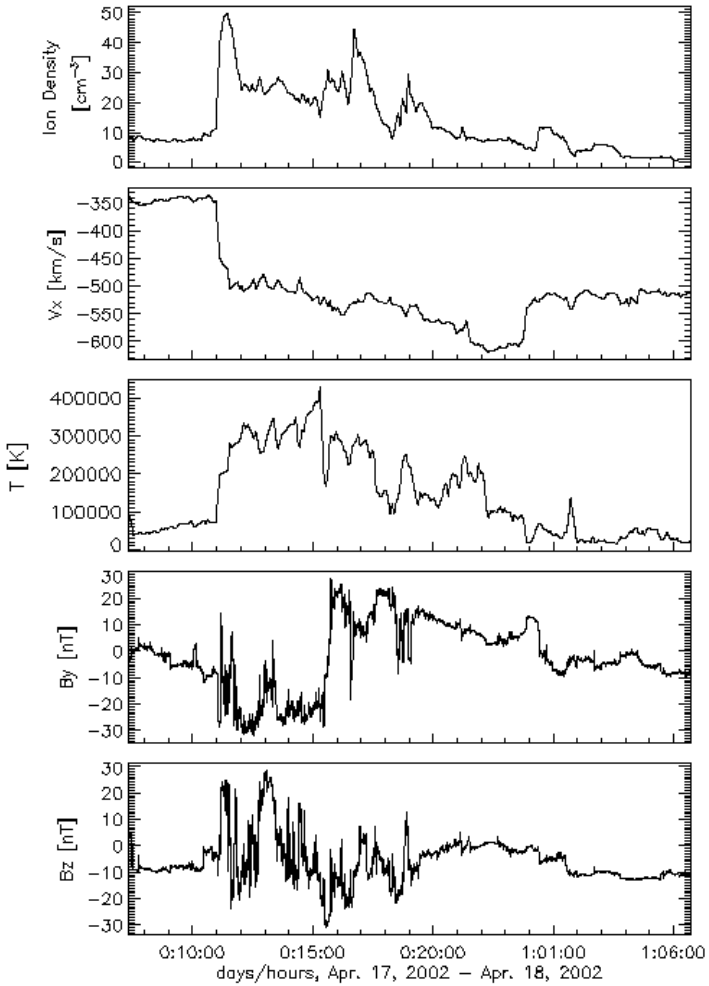

Density in the Magnetosphere

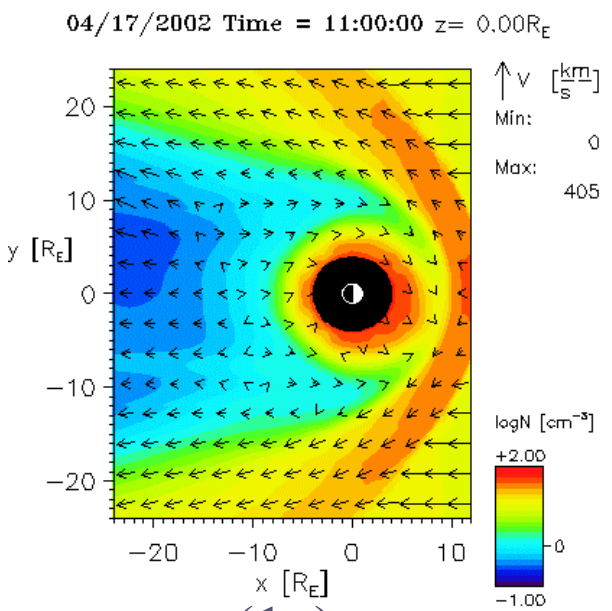

(1a)

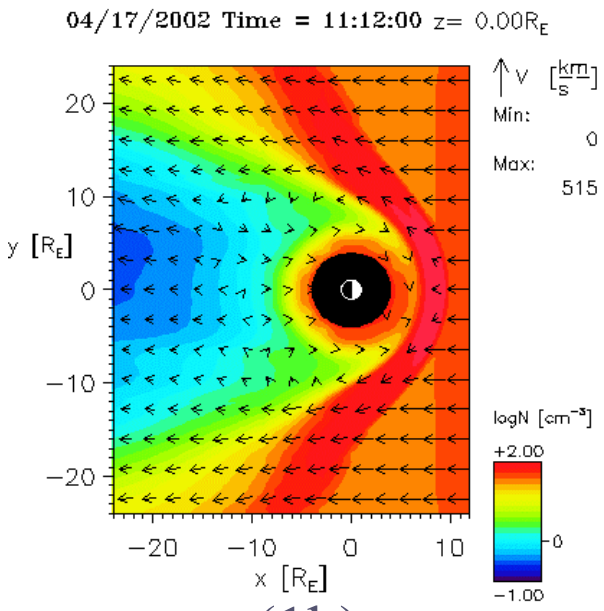

(1b)

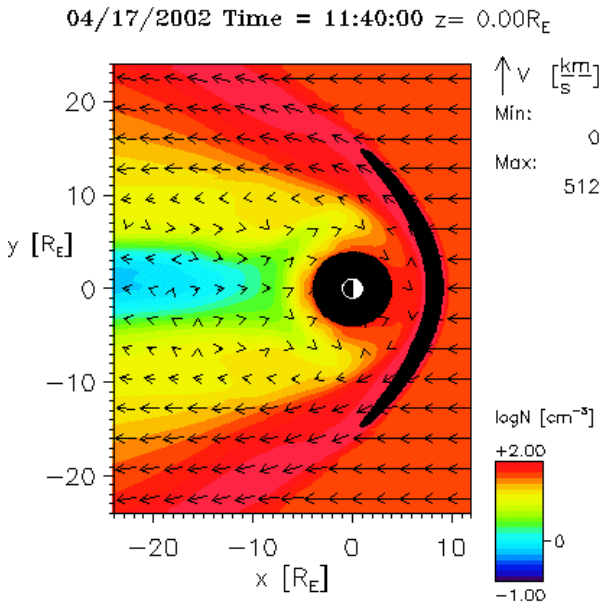

(1c)

- Figure 1a shows the density in the z=0 plane (GSM) before the shock hits.
- Figure 1b shows the compression of the magnetosphere at the beginning of the shock.
- Figure 1c shows the increase in the density in the tail as shock propagates down the tail.

Field-Aligned Currents (z=1 R_E GSM)

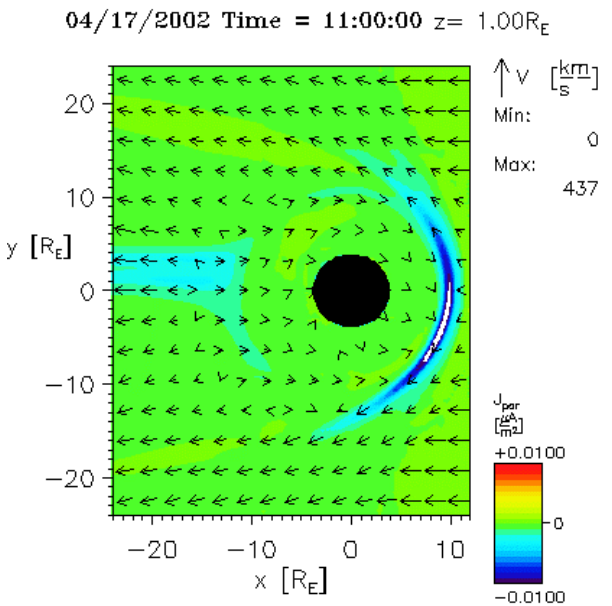

(2a)

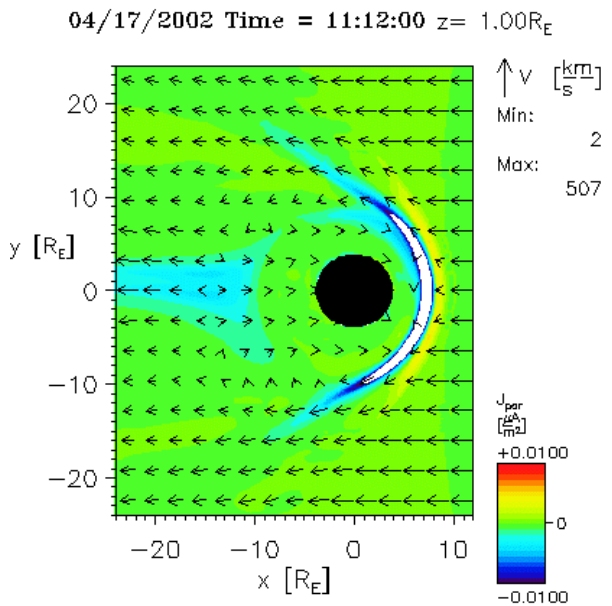

(2b)

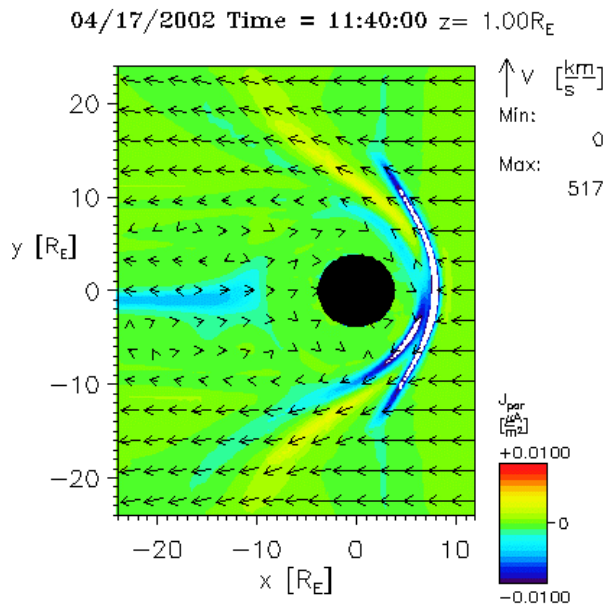

(2c)

- After the compression, increases in FACs can be seen on the dusk side magnetosphere and also near the magnetopause.

Currents and Potential in the Ionosphere

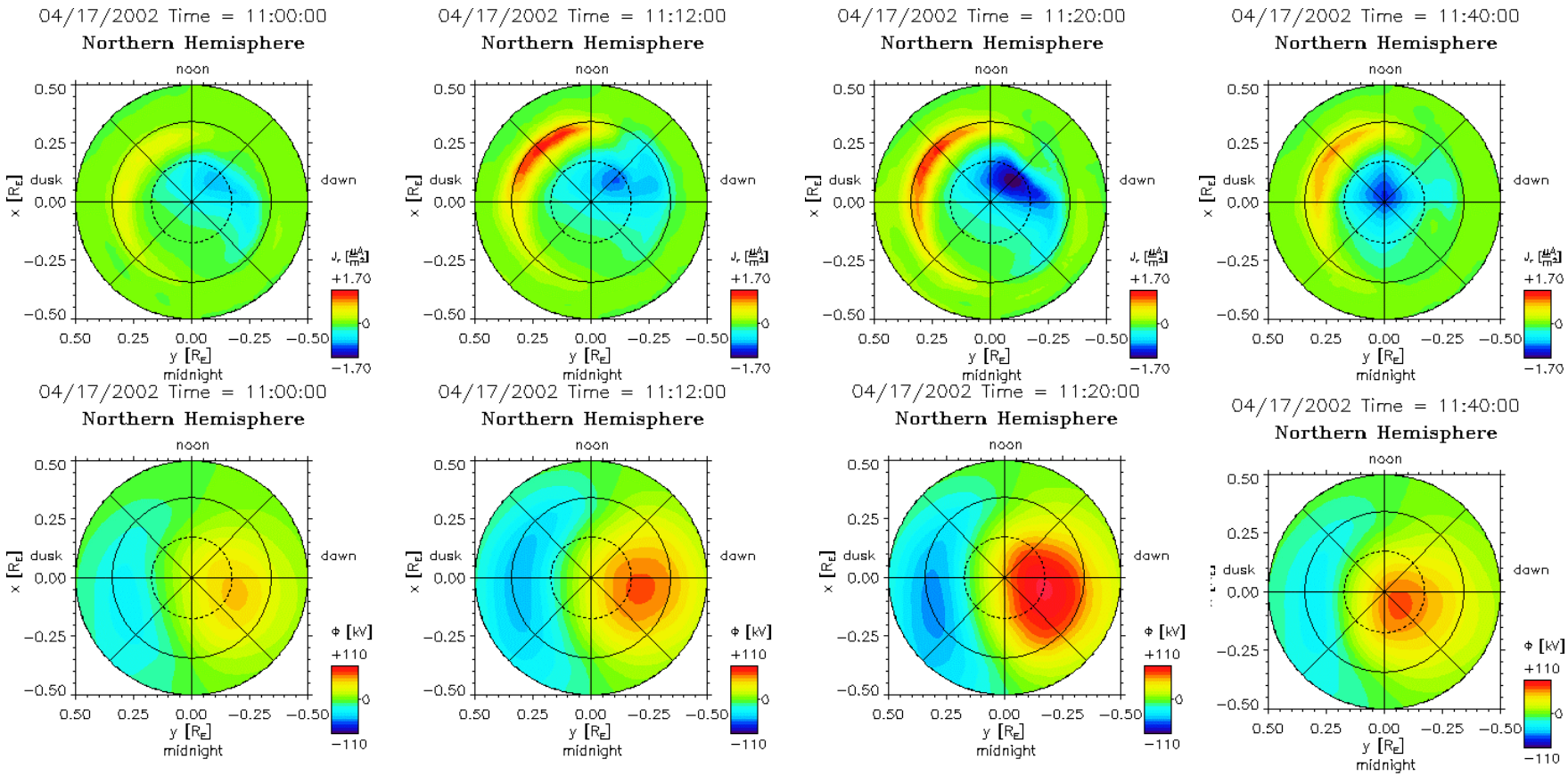

- The top row shows currents into and out of the ionosphere while the bottom row shows potential.
- The FAC increases on the dusk side of the ionosphere and also near the pole. The potential increases on the dusk side map to an area around x=-3.5 R_E and y = 9-10 R_E.

Cross Polar Cap Potential

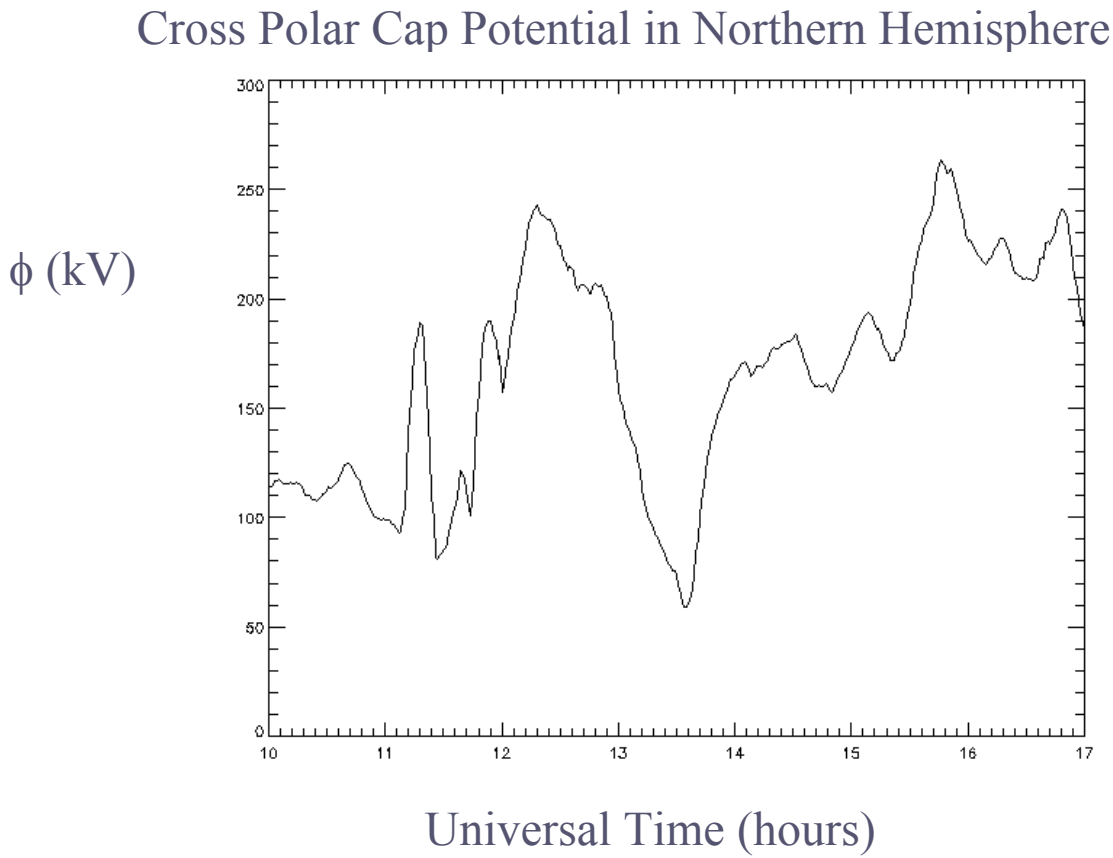

- There were three large potential increases that start around 11:08, 11:48 and 12:00.

Ring Current

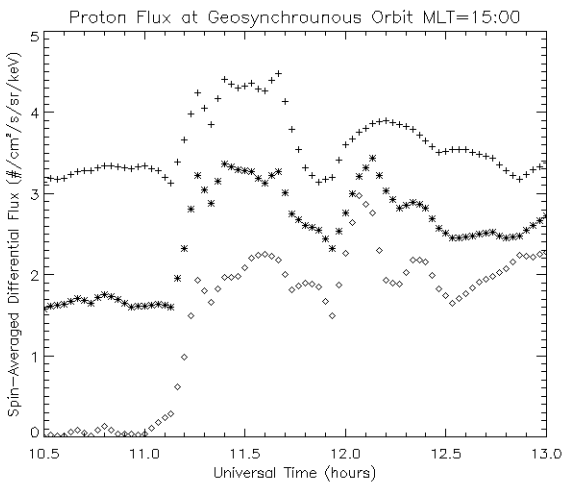

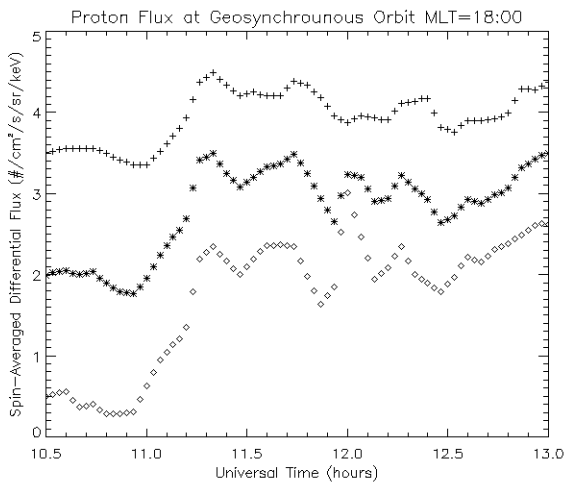

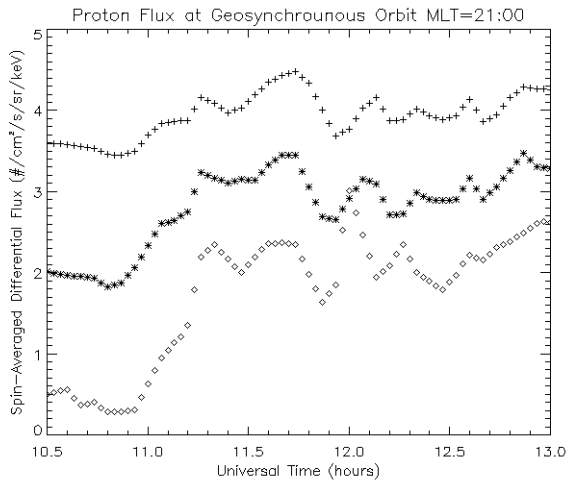

- The energy levels are 94(+), 141.5(*), and 210(◊) keV from top to bottom.
- The orbits are at 6.6 R_E at the z=0 plane (SM) at a fixed MLT.
- At 18 and 21 MLT, there was an increase in the flux starting before 11 UT then there was a larger increase starting around 11:12 UT.
- There was a large increase for 15 MLT starting around 11:08. The increases in flux were around 1.5-2 orders of magnitude.

Ring Current

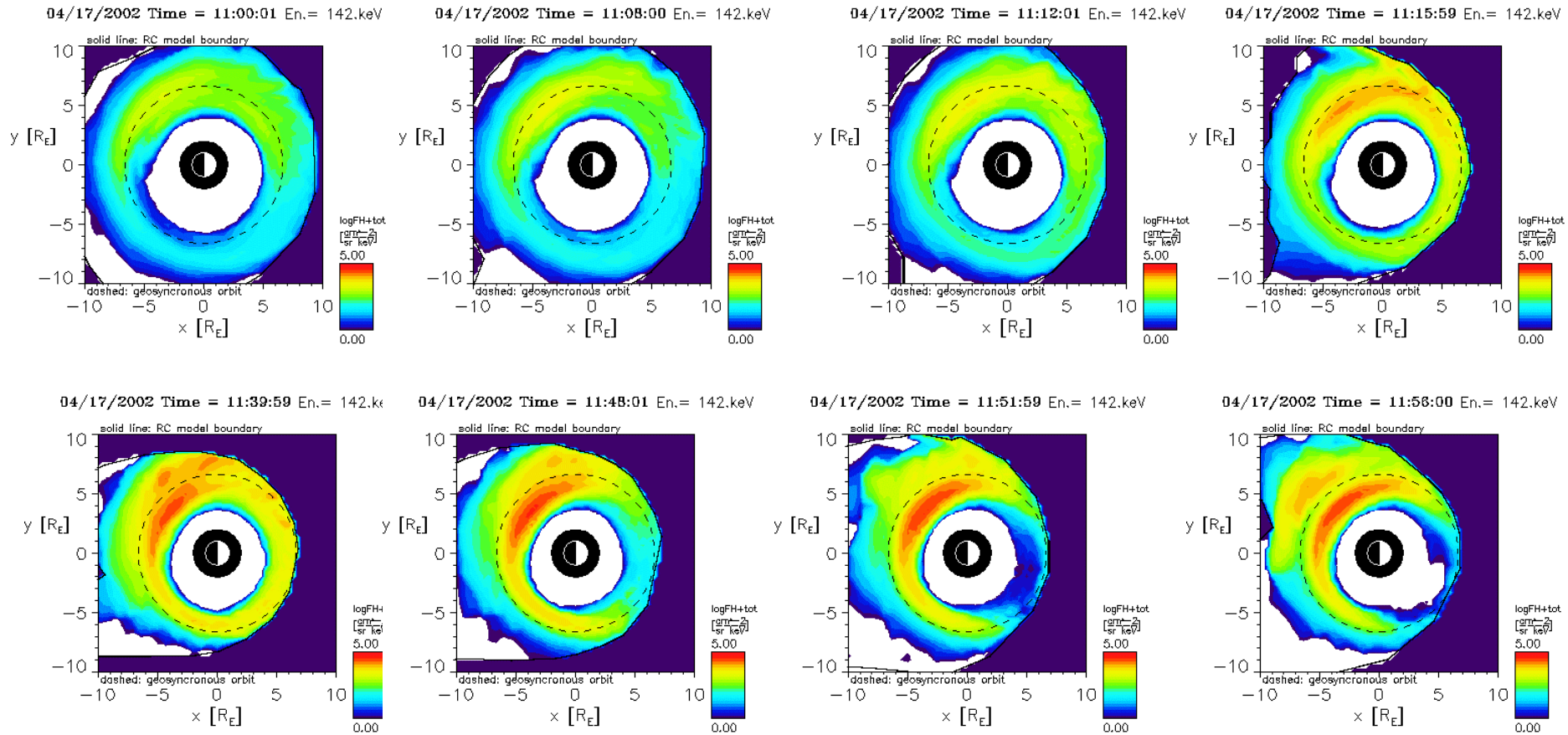

- The energy level is 141.5(*) keV. The plot is the z=0 plane (SM).
- Increases can be seen around 11:12, 11:40, and 11:52.

Density in the Tail

- The plot shows the density integrated from y=-5 to 5 R_E at x=-10 R_E and z=0 R_E.
- There were two large increases starting around 11:10 and 13:30.
- The first increase in density corresponded to an increase in the proton flux for higher energies (> 90 keV).
- The second increase corresponded to an increase in flux for a narrower range of energies. This can be seen in the 106 keV and 142 keV energy plots.

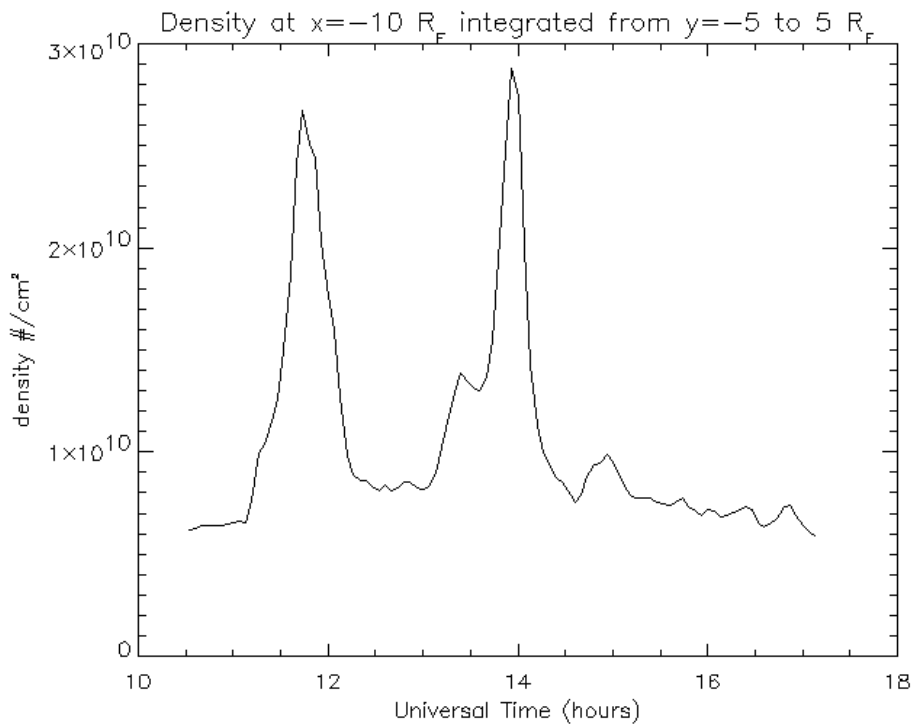

Ring Current

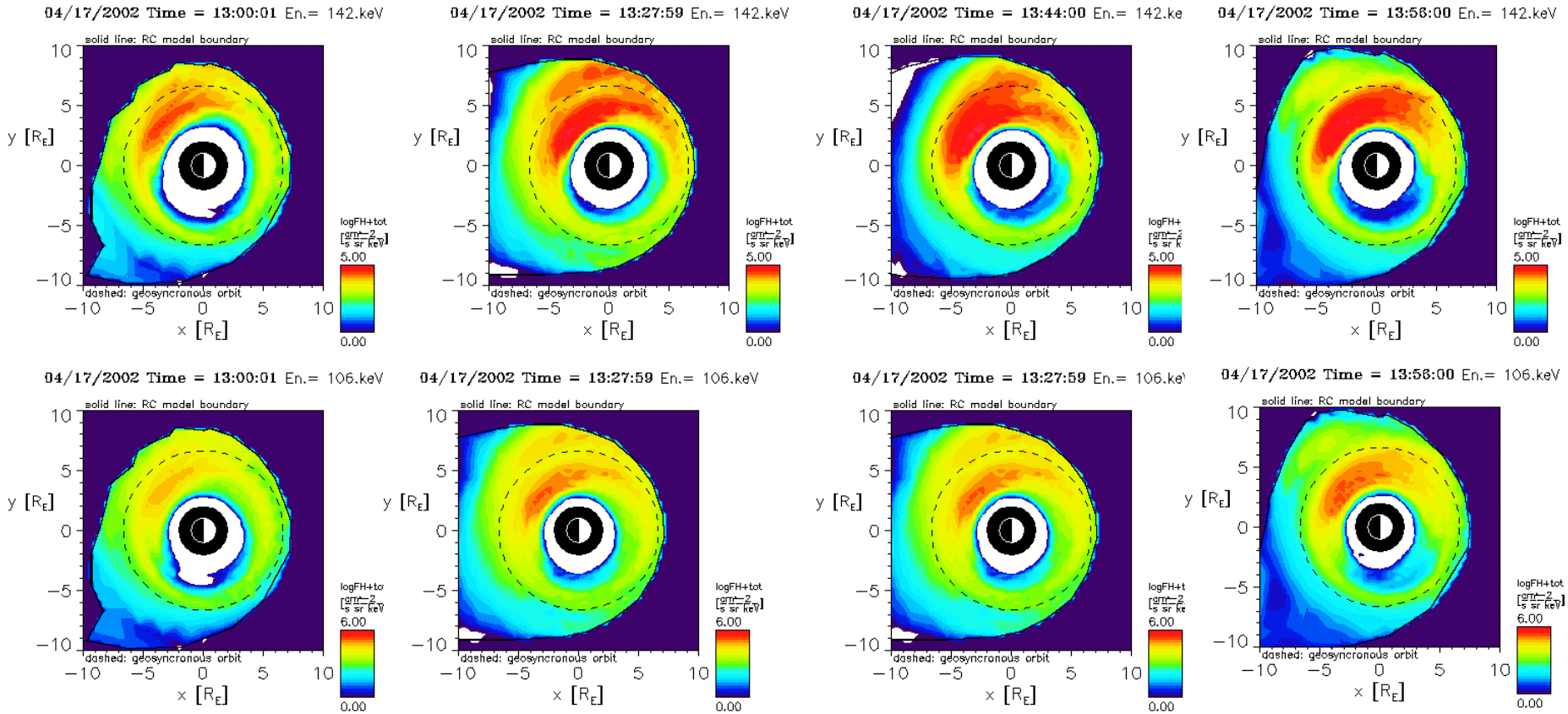

- An increase in flux can be seen in these two energies from 13:00 to 14:00.
- This corresponds to an increase in the density in the tail at x=-10 R_E but a relative minimum in the ionospheric potential.

Integrated Flux in Z=0 plane (SM)

- The pitch angle-averaged differential flux is integrated over the z=0 plane for each time step. Three energies are shown 106.4, 178.6 and 300 keV.
- At the two high energies, increases were seen around 11:12, 11:48, 12:48, 14:42 and 15:42.
- Three of these increases also correspond to increases in the cross-polar cap potential.
- The long decrease in flux after 13:00 for the two highest energies occurred at a time when the ionospheric potential was at a minimum due to the influence of strong IMF B_y.

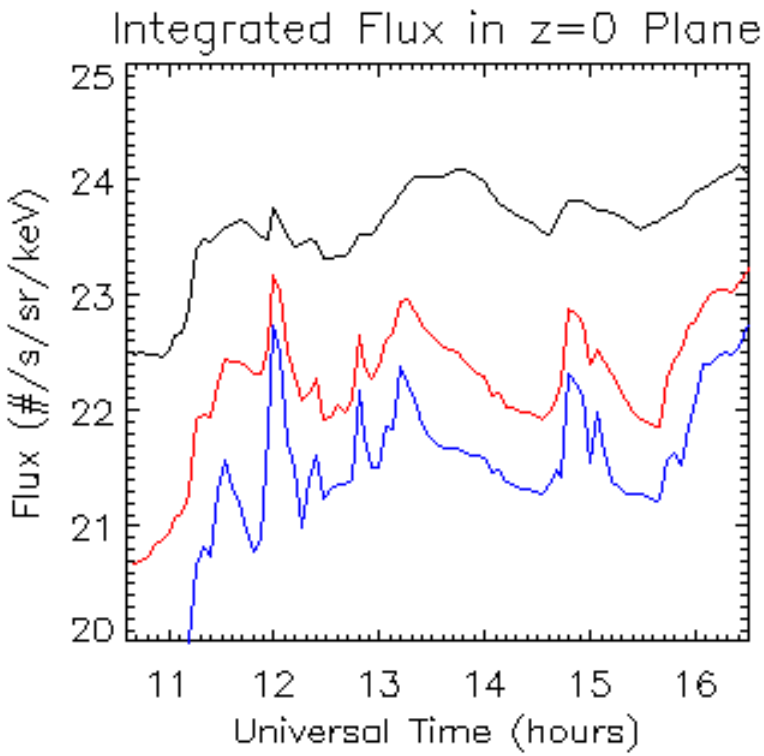

LANL Geosynchronous Proton Data

April 17, 2002

Spin-Averaged Differential Flux
(#/cm^2/s/sr/keV)

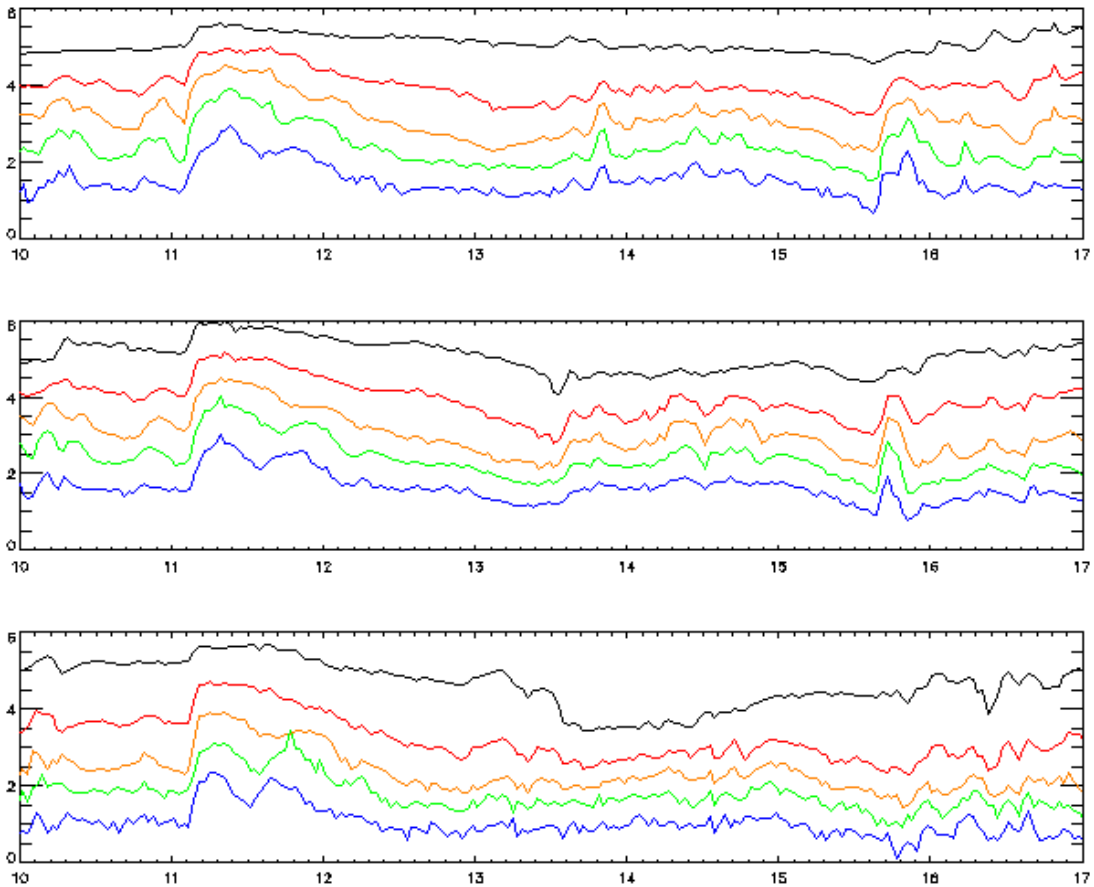

Universal Time (Hours)

LANL-97A
Geographic
Longitude
104

1994-084
Geographic
Longitude
145

1991-080
Geographic
Longitude
–165

Energies (keV):

50-75 black

75-113 red

113-170 orange

170-250 green

250-400 blue

Model Proton Flux

April 17, 2002

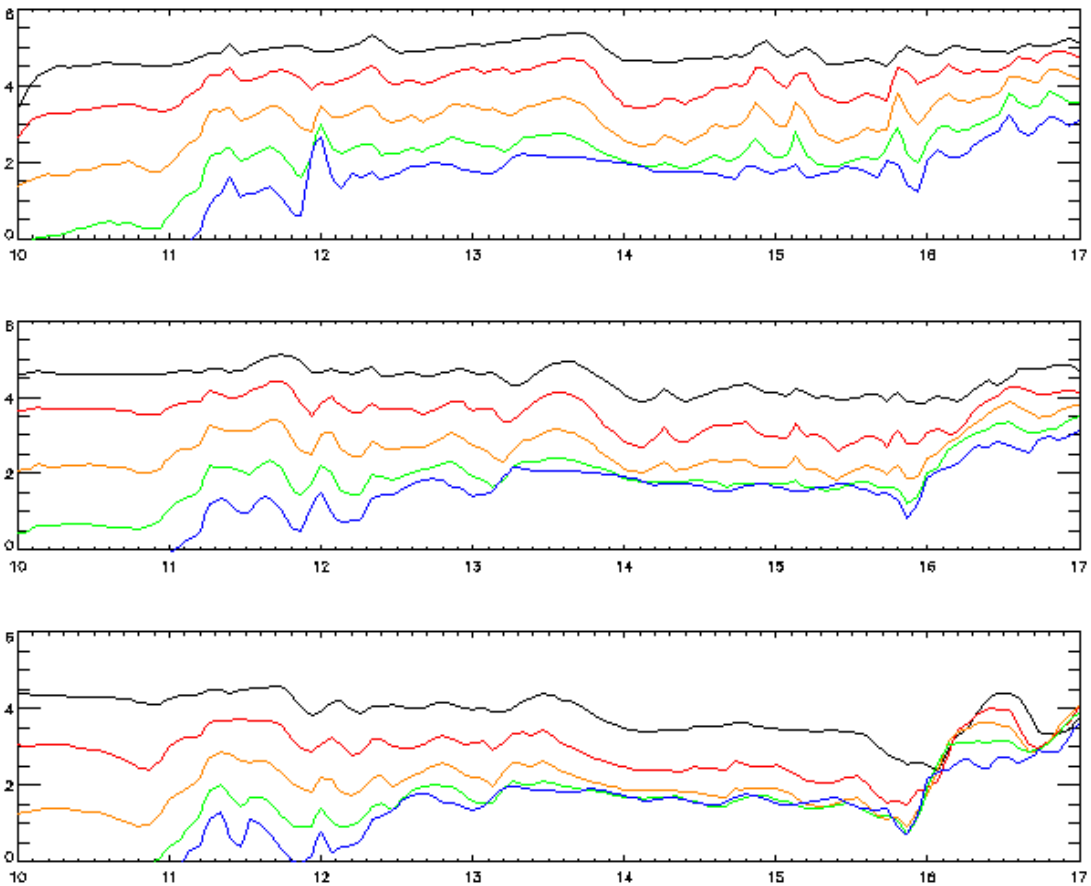

Energies (keV):

62.5 black

94 red

141.5 orange

210 green

300 blue

Ring Current

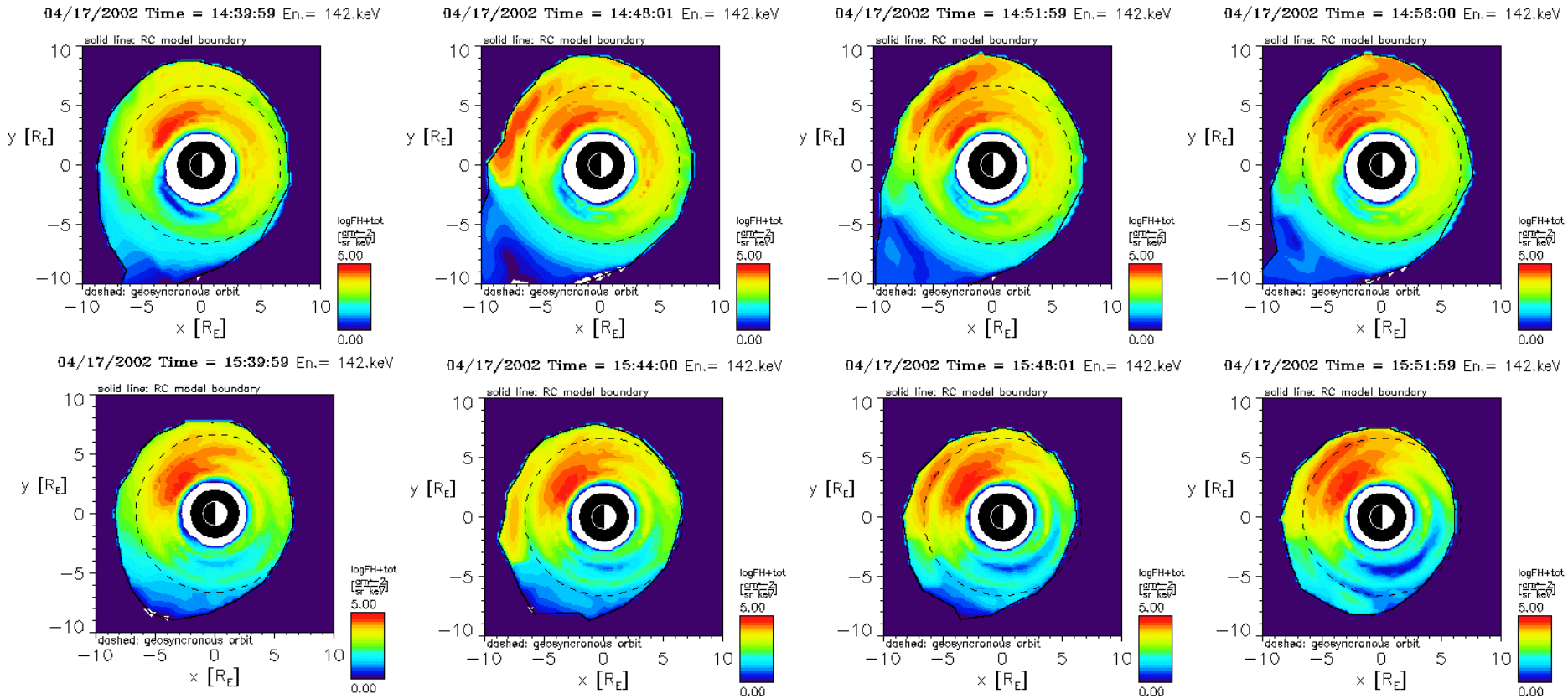

- An increase in the proton flux at geosynchronous orbit occurred at 14:52 and 15:48.
- The increase at 15:48 was also seen by the LANL satellites.

Ionospheric Potential

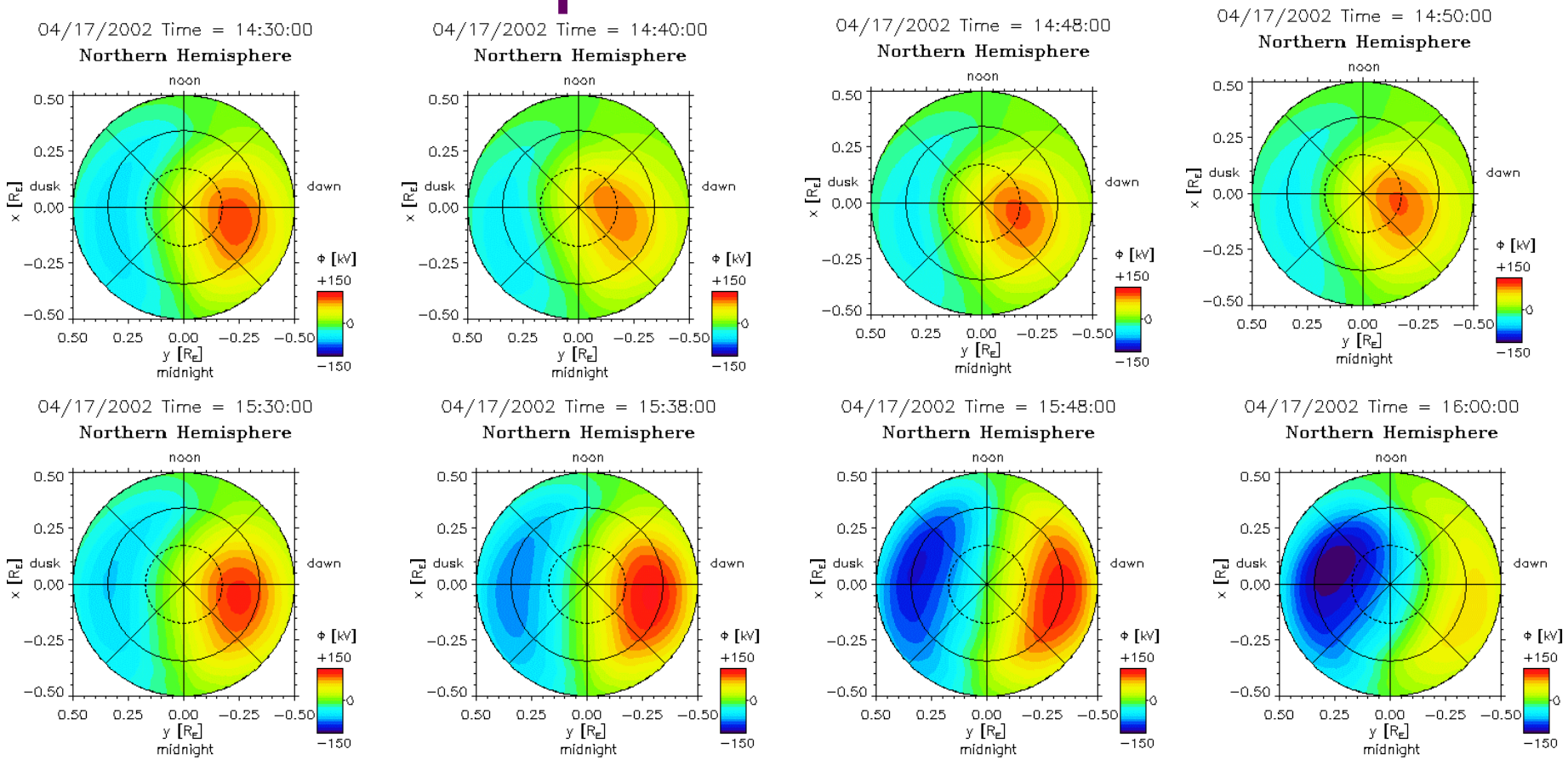

- Between 14:30 and 14:50 the potential changed only a little.
- Between 15:30 and 15:48, there was a large increase in the potential. After 15:48 the potential on the dawn side began to decrease.

Comparison between LANL data and model

- Both had increases in the flux around 11:12 and 15:40.
- In the LANL data, there were decreases in the flux seen by all three satellites with a minimum around 13:00 for two satellites and 13:30 for the other satellite.
- The model results from orbit calculations did not show a significant decrease. The calculation of the integrated flux showed a decrease but at a later time.

Discussion

- For the time period between 11:12 and 12:00, the increase in the proton fluxes seems to be driven by changes in the solar wind.
- The shock caused a large compression that increased the density in the magnetosphere and increased the potential in the ionosphere.
- The IMF increased and fluctuated in both B_z and B_y.
- Large increases in the proton flux in the model can be seen on the duskside. Increases in particle fluxes around 11:12 are seen in the LANL data.

Discussion

- The increases in the proton flux seen in the model occur mainly with increases in the potential. The flux increase seen at 14:48 does not have a significant potential increase but does have a small increase in the density in the tail.
- There was a large increase in density in the tail that did not have a corresponding increase in the integrated flux. This corresponded to a minimum in the potential under the influence of a strong IMF B_y.

Sawtooth Injections on April 18

LANL Data

Model

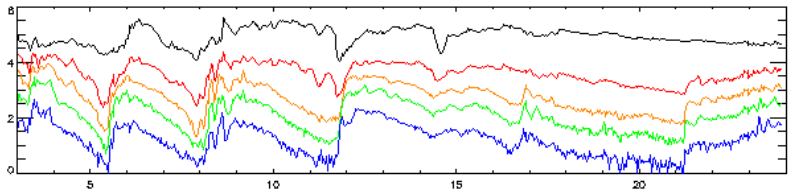

1991-080
Longitude
–165

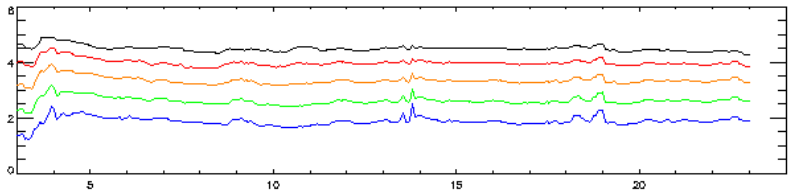

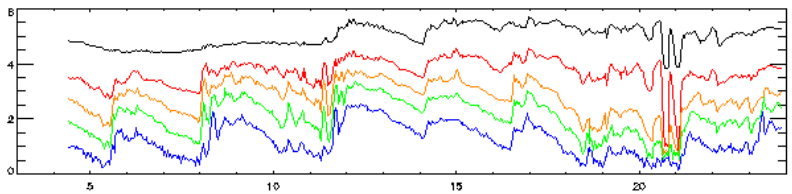

LANL-97A
Longitude
104

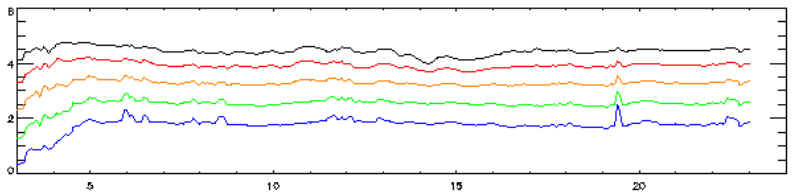

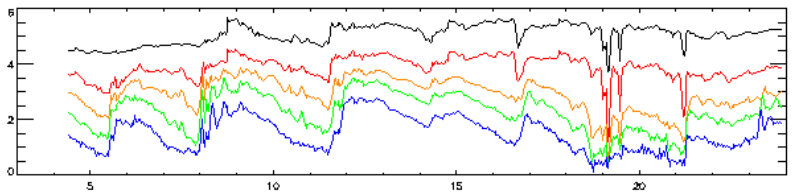

1994-084
Longitude
145

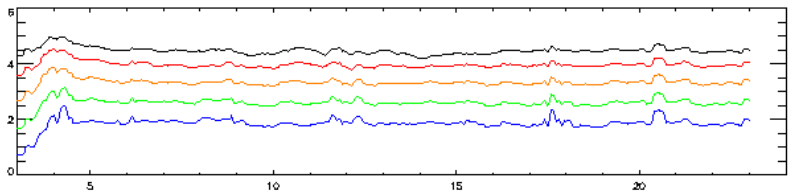

- The model got the amplitude approximately right but did not see the sawtooth injections.
- The solar wind conditions were relatively stable for this day and there was no large changes in the ionospheric potential to drive sawtooth injections.

Energies (keV): data 50-75 black 75-113 red 113-170 orange 170-250 green 250-400 blue
model 62.5 black 94 red 141.5 orange 210 green 300 blue

References

- Powell K. G., P. L. Roe, T. J. Linde, T. I. Gombosi, and D. L. De Zeeuw, A solution-adaptive upwind scheme for ideal magnetohydrodynamics, *J. Comput. Phys.*, 154(2), 284-309, 1999.
- Fok M.-C., T. E. Moore, and M. E. Greenspan, Ring current development during storm main phase, *J. Geophys. Res., 101,* 15,311-15,322, 1996.

Acknowledgments

- This work was performed while one of the authors (K.A.K) held a National Research Council Research Associateship at Goddard Space Flight Center.
- Geosynchronous proton flux data was provided by the Energetic Particle team at Los Alamos National Laboratory, Richard Belian (PI).
- ACE data was obtained through the CDAWeb. We thank the ACE SWEPAM instrument team and the ACE MAG instrument team for the data.